Multiperipheral theory of multiple particle production and experiment

I. M. Dremin

P. N. Lebedev Physics Institute, Moscow

Fiz. Élem. Chastits At. Yadra **6**, 45–71 (January–March, 1975)

The development of multiperipheral schemes is briefly reviewed. The correspondence between the various models employed is demonstrated. General qualitative results of the multiperipheral theory, and their possible applications, are discussed. Applications of the theory to the description of particular experiments are considered.

PACS numbers: 12.40.S, 13.80.K

INTRODUCTION

The multiperipheral theory has served as the principal scheme for describing inelastic interactions of high-energy particles for more than a decade. So far, however, it is more readily successful in the qualitative rather than in the exact and complete quantitative description of these processes, although it should be noted that the application of the simplest variants to particular reactions has been quite successful. Moreover, even the qualitative features of the multiperipheral scheme can change form when its more complicated variants are considered. In any case, however, this scheme points the way towards classification of many-particle events and the choice of the variables for their description. The use of the unitarity condition makes it possible to reveal with the aid of the same scheme also the main characteristics of elastic scattering, thus relating the scheme with the Regge approach.

We consider below all these aspects of the multiperipheral model, with particular emphasis on the debatable or still incompletely developed problems.

The multiperipherism idea itself consists of a natural generalization of the concepts concerning the peripheral hadron interaction.[1–3] The development of these ideas has made considerable progress after the introduction of Feynman diagrams with one-meson exchange[4,5] and after formulation of the one-meson approximation. An essential attractive feature of the multiperipheral approach is that while it combines all the physical ideas of the one-meson approximation, it is based on a more powerful mathematical foundation, namely an integral equation[8] whose solution leads to conclusions concerning the character of the inelastic and elastic particle interaction processes. It is very important here that the integral equation can be obtained from the general field-theoretical Bethe–Salpeter equation,[9] with the aid of which it is possible to obtain a consistent interpretation of the kernel of the equation as the aggregate of a definite class of Feynman diagrams, and consequently understand the connection between the different multiperipheral schemes employed. We emphasize that the kernel of the integral equation of the multiperipheral theory is not determined by the main premises of the theory, and is chosen only phenomenologically. It becomes necessary here to make definite assumptions concerning certain quantities, and a number of the parameters must be left arbitrary until a comparison is made with experiment. Nonetheless, even during this stage it is possible to explain the qualitative and in some cases also the quantitative characteristics of the inelastic processes and to connect them with the properties of the amplitude of the shadow elastic scattering. This connection turns out to be very fruitful, since the characteristic of elastic scattering (and of the associated optical theorem for the total cross section) are known most accurately and can be used to determine the parameters of the model. All the predictions concerning the inelastic processes can now be made using already a much smaller number of free parameters. At present, to prove the viability of one multiperipheral model or another it is necessary not only to describe the main qualitative features of the experimental data, but also to compare a large number of theoretically calculated quantitative characteristics with experiments on elastic and inelastic processes.

1. CORRESPONDENCE BETWEEN VARIOUS MULTIPERIPHERAL SCHEMES

The connection between various multiperipheral models will be demonstrated within the framework of a single approach, based on the Bethe–Salpeter equation. We consider for simplicity the interaction of two pions. The elastic-scattering amplitude A satisfies the equation

$$A(s, t, p_{1,3}^2) = \bar{A}(s, t, p_{1,3}^2) - \frac{i}{2(2\pi)^4}\int d^4k_1 \bar{A}(s_1, t, p_{1,3}^2, k_{1,2}^2) \times A(s_2, t, k_{1,2}^2) D(k_1^2) D(k_2^2), \quad (1)$$

which is shown graphically in Fig. 1, where all the particle momenta p_i are indicated; $s = -(p_1 + p_2)^2$; $t = -(p_1 + p_3)^2$; $s_1 = -(p_1 - k_1)^2$; $s_2 = -(p_2 + k_1)^2$; $k_2 = p_1 + p_3 - k_1$; $\bar{A}$ stands for the irreducible (in the t-channel) part of the amplitude[1]; $D(k_i^2)$ are the propagation functions $[D(k^2) = (k^2 + \mu^2)^{-1}$, where μ is the pion mass$]$.

Expanding the amplitude in partial waves in the t-channel:

$$A(s, t, k_i^2) = \sum_{l=0}^{\infty} (2l+1) f_l(t, k_i^2) P_l(z) \quad (2)$$

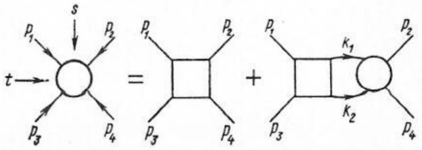

FIG. 1. Diagram form of the equation for the elastic-scattering amplitude.

Copyright © 1976 American Institute of Physics

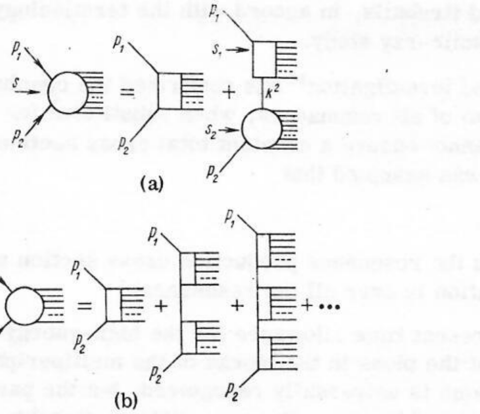

FIG. 2. Equation for the total cross sections; a) diagram representation, b) iteration solution.

(the expansion for $\bar{A}$ is analogous) and regularizing the behavior of the partial waves at the threshold by introducing the functions

$$\varphi_l = (2|\mathbf{k}_1|^2)^{-l}(t-4\mu^2)^{-l/2} f_l, \tag{3}$$

it is easy[9] to obtain from (1) an equation for the partial amplitudes; at $t=0$ this equation is

$$\varphi_l^I(p^2) = \bar{\varphi}_l^I(p^2) + \frac{2^{2l-1}\sqrt{\pi}\,\Gamma(l+3/2)}{(2\pi)^3\Gamma(l+2)} \times \int \frac{dk^2\,(k^2)^{l-1}}{(k^2+\mu^2)^2}\bar{\varphi}_l^I(k^2, p^2)\,\varphi_l^I(k^2). \tag{4}$$

where $p^2=p_1^2=p_3^2$; $k^2=k_1^2=k_2^2$; I is the isospin in the t-channel.

Using the inverse Sommerfeld-Watson transformation

$$\varphi_l^I = (4pk)^{-l}\frac{2}{\pi}\int_{z_{\min}}^{\infty} A_1^I Q_l(z)\,dz, \tag{5}$$

it is easy to obtain the following equation for the imaginary part of the amplitude at $t=0$:

$$A_1^I(s, p^2) = \bar{A}_1^I(s, p^2) + \frac{1}{32\pi^3|\mathbf{p}|\sqrt{s}}\int dk^2\,ds_1\,ds_2 \times \frac{\bar{A}_1^I(s_1, p^2, k^2)\,A_1^I(s_2, k^2)}{(k^2+\mu^2)^2}. \tag{6}$$

The integration region in (6) is determined by the conditions

$$\begin{gathered}-k^2[(s+p^2-\mu^2)^2-4p^2\mu^2]+(s_1-p^2+k^2)^2\mu^2-p^2(s_2-k^2-\mu^2) \\ -(s_1+p^2+k^2)(s_2-k^2-\mu^2)(s+p^2-\mu^2)\leqslant 0, \\ s_{1,2}\geqslant 4\mu^2,\ \sqrt{s}\geqslant\sqrt{s_1}+\sqrt{s_2}\end{gathered} \tag{7}$$

With the aid of the optical theorem

$$A_1(s, p^2) = \sigma(s, p^2)\sqrt{(s+p^2-\mu^2)^2+4\mu^2p^2} \tag{8}$$

we obtain from (6) an equation for the total cross section $\sigma(s, p^2)$:

$$\sigma(s, p^2) = \bar{\sigma}(s, p^2) + \frac{1}{16\pi^3}\int dk^2\,ds_1\,ds_2\,D^2(k^2)\,\bar{\sigma}(s_1, p^2, k^2)\,\sigma(s_2, k^2)\,H, \tag{9}$$

where

$$H = \frac{[(s_1+p^2-k^2)^2-4p^2k^2]^{1/2}[(s_2+k^2-\mu^2)^2+4k^2\mu^2]^{1/2}}{[(s+p^2-\mu^2)^2+4\mu^2p^2]}. \tag{10}$$

Equations (4), (6), and (9) are the fundamental equations used in the theoretical description of the inelastic processes (9) and the singularities of the partial amplitudes of the shadow elastic scattering in the crossing channel (4).

Equation (9) was first derived in Ref. 8, although its representation in the form of an iteration series was used even earlier.[18] The diagram representation of this equation for inelastic processes, and also its iteration solution, are given in Fig. 2. The rectangles in this figure show the irreducible term and the kernel of this equation, which describe non-one-meson nonperipheral processes.[2)] The integral term of the equation is the total cross section of the peripheral processes, i.e., processes due to one-meson exchange.

Usually Eq. (9) and the method of its derivation raise a number of questions, principal among which are the following: Why is the pion chosen as the exchanged particle, rather than some other particle (possibly also a reggeized one), and in what form should one choose $\bar{\sigma}$ (or, equivalently, $\bar{A}_1$)?

It must be stated that various multiperipheral models differ precisely in the fact that their answers to these two questions are different. Their assessment can therefore establish the correspondence between the various schemes.

In principle, an equation of the type (9) can be written down purely formally by choosing as the basis diagrams with exchange of any mesons. Such an equation, however, would have two unfavorable features in comparison with (9): First, the kernel of the equation would be determined by the cross section for the interaction of those mesons about which we know much less than about pion interaction. Second, the presence of a much larger mass than the pion mass in the propagators in the integral term would greatly reduce the role of this term and make the conditions of the problem worse, since the total cross section would be specified to an ever increasing degree by an inhomogeneous term of the equation, which would be chosen *ad hoc*. Allowance for non-one-pion exchanges will therefore be made in $\bar{\sigma}$, and by the same token the entire problem will be reduced to the second question.

The choice of a reggeized exchange pion, while sometimes useful, does not change the main results. It does, however, complicate Eq. (9) appreciably, since this equation goes over into the so-called Chew–Goldberger–Low equation.[12] The only noticeable difference between the results and those obtained in the case of nonreggeized exchange lies in the distribution with respect to the Treiman–Yang angle,[13] which now becomes anisotropic.

All the other distributions in which integration is carried out with respect to this angle can be made the same in both cases by suitable choice of the behavior of $\bar{\sigma}$ off the mass shell.[11,14]

The quantity $\bar{\sigma}$ is the stumbling block of all the multiperipheral schemes. All we know about it is that it is necessary to take into account here all the nonperipheral (non-one-meson) diagrams. This requirement, however, is not too specific and affords a great leeway in the choice of the form of the function $\bar{\sigma}(s, p^2, k^2)$. This function is chosen phenomenologically. The difference between the numerous models lies in the differences in the behavior of $\bar{\sigma}$ as a function of s and k^2. The main parameters that arise in this case are connected with the asymptotic form with respect to s and with the rate of decrease as a function of k^2.

In particular, if

$$\bar{\sigma} \sim s^{\bar{l}-1} \quad \text{as} \quad s \to \infty, \tag{11}$$

then one of these parameters is $\bar{l}$, which in the language of partial waves is connected with the approximation of the irreducible partial amplitude in the form of a pole at the point $l = \bar{l}$. The multiperipheral equations can be made self-consistent only if $\bar{l} < 1$ (we shall return to this question later).

The dependences on s and k^2 are usually chosen either factorized, of the type

$$\bar{\sigma}(s, k^2) = \bar{\sigma}(s, k^2 = -\mu^2) F(k^2), \tag{12}$$

where $F(k^2)$ is assumed to decrease with increasing k^2, or else in schemes with exchange of reggeized particles in the usual Regge form

$$\bar{\sigma}(s, k^2) \sim s^{\alpha(k^2)} \sim \exp[\alpha(k^2) \ln s], \tag{13}$$

where $\alpha(k^2)$ is chosen such that $\bar{\sigma}$ decreases with increasing k^2 at large k^2. Over a small interval of variation of s, the difference between (12) and (13) is also small. Therefore the main parameter in (12) and (13) is the effective value of k^2 over which a noticeable decrease of the kernel $\bar{\sigma}$ takes place with increasing k^2.

The simplest model was proposed first by Amati *et al.*[8] The main results of the model (Regge behavior, scaling, etc.) are well known. In this model the peripheral processes consist only of low-energy pion interactions, and in particular, of the production at each node of the diagram of one resonance, namely the ρ meson. The necessary condition of the model is that the cross section $\bar{\sigma}$ be integrable with respect to s:

$$\int_{s_{\min}}^{\infty} \bar{\sigma}(s)\, ds < \infty, \tag{14}$$

i.e., $\bar{l} < 0$. Owing to such a rapid decrease with energy, the dependence on k^2 was neglected, i.e., it was assumed that $F(k^2) \equiv 1$, meaning that the interaction off the mass shell is the same as for real pions.

The main shortcoming of this model is that the total cross section decreases with increasing energy (asymptotically not slower than $s^{-0.7}$), in contradiction to the experimental data at high energies. As shown in Ref. 9, this is due to the smallness of the numerical factor in front of the integral term of the equation for the total cross section, a factor that appears as a result of the propagation function of the exchanged virtual particle. Constancy of the total cross section can be attained only if $\bar{\sigma}$ is large enough even outside the region of the resonances at $s \sim 10\ \text{GeV}^2$, i.e., if a noticeable contribution is made by events with production of large-mass pion systems (approximately up to 3 GeV). Since such pion systems have been observed in the interaction of cosmic rays,[15] the theoretically observed pion groups were called fireballs, in accord with the terminology used in cosmic-ray study.

A detailed investigation[16] has confirmed the conclusion that the sum of all resonances, when substituted for $\bar{\sigma}$ in (9), cannot ensure a constant total cross section. In Ref. 16 it was assumed that

$$\bar{\sigma} = \sum \bar{\sigma}_r, \tag{15}$$

where $\bar{\sigma}_r$ is the resonance production cross section and the summation is over all the resonances.

At the present time allowance for the high-energy interaction of the pions in the blocks of the multiperipheral diagrams is universally recognized, but the particular ways of making this allowance differ noticeably from one another.

Thus, in some papers[17–19] it is proposed to add to the sum of all the pion resonances the cross section of only the elastic interaction of the pions at high energies, i.e., to assume that

$$\bar{\sigma} = \sum \bar{\sigma}_r + \bar{\sigma}_d, \tag{16}$$

where $\bar{\sigma}_d$ is the cross section for the elastic diffraction scattering at high energies. In this case, by suitable choice of the parameters, it is possible to obtain practical constancy of the total cross section in a wide energy interval.[17] We note, however, that the form factor $F(k^2)$ [see (12)] chosen in Ref. 17 is much larger than unity in a wide range of values of k^2, and differs in its behavior from all the experimentally known form factors. Nevertheless, even with such a "growing" form factor it is impossible to obtain the required value of the total cross section (the value $\sigma = 12$ mb which is the starting point in Ref. 17), and a low average multiplicity of the processes is obtained.

Consequently, the non-one-pion inelastic processes should become important, i.e., at high energies $\bar{\sigma}$ should receive contributions not only from elastic scattering but also from the inelastic interactions[20]:

$$\bar{\sigma} = \sum \bar{\sigma}_r + \bar{\sigma}_d + \bar{\sigma}_b, \tag{17}$$

where $\bar{\sigma}_b$ is the cross section of inelastic non-one-pion processes. We note that it is precisely this contribution $\bar{\sigma}_b$ which was set in correspondence with the fireball-production processes in Ref. 9. In connection with the experimental indications that the angular distribution of the fireball decay products is nearly isotropic in the fireball proper reference frame, the hypothesis was advanced (to which we shall return later) that the corresponding inelastic processes in $\bar{\sigma}$ have a statistical character, and if their contribution $\bar{\sigma}_b$ does depend on the energy at all, the dependence is extremely weak.

Another assumption used in Refs. 21–23 is that the

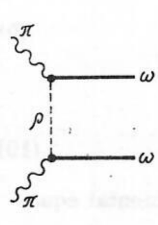

FIG. 3. Example of diagram with non-one-pion exchange.

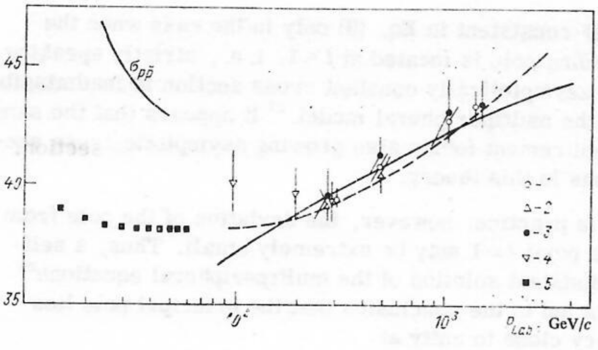

FIG. 4. Dependence of the total pp-interaction cross section on the energy. The figure shows the pp-interaction cross sections at energies up to 70 GeV: 1—CERN—Rome; 2—CERN—Rome (Coulomb); 3—Pisa-Stony Brook; 4—NAL; 5—Serpukhov; ------ $\sigma = 38 + 0.68 \ln^2(p/100)$; ——— $\sigma = 60[1 - 3/(\ln p + 3)]$.

inelastic processes that enter in $\bar{\sigma}_b$ are due to single-particle (but not to one-pion) exchange, and that the interaction of the virtual exchanged resonances, which are assumed reggeized in Refs. 21—25, leads to the production of single real particles or resonances. The diagram form of this hypothesis is shown in Fig. 3, where one of the diagrams contributing to $\bar{\sigma}_b$ in the case of $\pi\pi$ interaction is shown by way of example. We note that as a result of this assumption the elastic scattering of the pions makes no contribution to $\bar{\sigma}$ at high energies, i.e., $\bar{\sigma}_d = 0$ in (17).

Thus, the number of models used in the multiperipheral approach is large. We have touched upon here only on those that claim to describe at least the main qualitative regularities that are deduced from the experimental data. In the next section we consider the conclusions and results of these models and their agreement with experiment.

2. EXPERIMENTAL DATA AT HIGH ENERGIES AND THEIR DESCRIPTION BY THE MULTIPERIPHERAL THEORY

Energy dependence of the total cross sections. At the present time the behavior of the proton-proton interaction cross section[24] is known over a very wide energy interval (Fig. 4). The decrease of the cross section in the interval from 10 to 30 GeV gives way to a plateau at energies 30—70 GeV, and at high energies the cross section is seen to have an increase, which reaches approximately 12% of the plateau level at 1500 GeV. The behavior of the cross section of the other processes (pion-proton, kaon-proton, etc.), which is known up to 70 GeV, is similar to the proton-proton cross section and is usually attributed to exchange of the leading poles in the t-channel and to cuts in conjunction with a family of poles at $l_0 \approx 0.5$ in the l plane. This explanation predicted also (see, e.g., Ref. 25) a pre-asymptotic growth of the cross section which was much less than that observed in experiment (compare the coefficients of the terms of type $\ln^{-1}p$ in Fig. 1 with those in Ref. 25). At the same time, in some theoretical models (e.g., in the eikonal model with exchange of vector or tensor particles[26]), an asymptotic growth of the total cross sections was predicted.

It is therefore of interest to ascertain whether the asymptotic region has been reached with the CERN colliding beams, or whether these are still pre-asymptotic data. In my opinion, there are enough convincing arguments for assuming that the asymptotic values have not yet been reached. The simplest argument is that the observed growth is still much smaller than the cross section in the region of the plateau, i.e., in all the theoretical approximations with increasing cross section the term that is leading from the point of view of increase with energy has not yet become numerically the principal one [as e.g., in the formula that yields a cross section that increases as $\ln^2 p$ (see Fig. 4)]. It is therefore still impossible to speak of the asymptotic region in the rigorous sense. One can imagine, however, a situation in which there is a dependence of the type shown in Fig. 4 both in this energy region and at still higher energies, i.e., the formula

$$\sigma = 38 + 0.68 \ln^2 (p/100) \tag{18}$$

will hold true also in the asymptotic limit.[3)] In this case the asymptotic formulas should hold true at these values of the energy also for other quantities, for example for the slope of the diffraction peak. There is, however, a close connection between the behavior of the total cross section and the slope of the diffraction peak. If we define the slope $b(s)$ of the peak by the relation

$$d\sigma/dt = (d\sigma/dt)_{t=0} \exp[b(s)t], \tag{19}$$

where $d\sigma/dt$ is the differential cross section for elastic scattering, and if it is recognized that the optical theorem leads to the relation

$$(d\sigma/dt)_{t=0} = \sigma^2(1+\Delta^2)/16\pi, \tag{20}$$

[where Δ is the ratio of the real elastic-scattering amplitude to its imaginary part at $t=0$], then integration of (19) yields

$$16\pi b(s)\sigma_{el} = \sigma^2(1+\Delta^2). \tag{21}$$

where σ_{el} is the total elastic-scattering cross section. Owing to the obvious relation $\sigma_{el} < \sigma$ we have

$$\sigma < 16\pi b(s). \tag{22}$$

Although this limitation is very weak numerically, it does follow from (22) that the slope of the peak $b(s)$ cannot increase asymptotically more weakly than the total cross section, i.e., if the asymptotic behavior already sets in in the total cross section and terms of the type $\ln^2 p$ do appear, then the same regularities should ap-

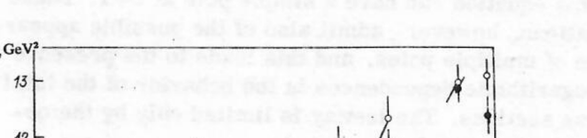

FIG. 5. Energy dependence of reciprocal diffraction-peak width: 1) Beznogikh *et al.*; 2) Amaldi *et al.*; 3) Barbiellini *et al.*

pear also in the $b(s)$ dependence. Experiment points to the opposite situation (Fig. 5): if the slope increases logarithmically to 70 GeV, then at higher energies this growth not only fails to increase, but even slows down. It follows from all this that the energies attained at ISR are still pre-asymptotic.

How is this pre-asymptotic behavior to be treated and what behavior of the cross sections can be expected here?

The most detailed quantitative estimates have been made in the Regge approach mentioned above. Here the growth of the cross sections in the pre-asymptotic region is due to the damping out, like $\ln^{-1}p$, of the negative corrections to the main term. But the growth of the cross sections turns out to be much larger (if the experimental data do not change) than the theoretically obtained result.[25] Asymptotically, on the other hand, the total cross sections decrease here in power-law fashion, with a small exponent. A regime of this type appears also in the multiperipheral theory. We shall discuss it later, and note here only that in the eikonal approximation there is an example of a very interesting regime,[26] where the total cross section in the pre-asymptotic region increases like $\ln^2 s$, but in the asymptotic region this regime turns into a superweak growth of the ln ln$s$ type. The slope of the diffraction peak increases weakly here even in the pre-asymptotic region, and becomes almost constant. This picture agrees qualitatively with the experimentally observed results.

It is impossible to distinguish, by means of the energy dependence, the asymptotic predictions of the Regge approach, with allowance for cuts, from the superweak regime obtained in the asymptotic region. There is, however, a numerical difference, owing to the different behavior in the pre-asymptotic region. Namely, whereas in the Regge approach the cross section at 10^6 GeV is approximately 60 mb, in the eikonal variant it rises to 100–120 mb at the same energies. Thus, the predictions in these cases differ significantly from each other, and in principle this is experimentally verifiable.

The equations of the multiperipheral approach, as shown already in Ref. 8, admit of a power-law behavior of the amplitude A_1 as a function of the energy s, and consequently admit of a power-law energy dependence of the cross sections. From the point of view of Eq. (4) for the partial amplitudes, this means that the solution of this equation can have a simple pole at $l<1$. These equations, however, admit also of the possible appearance of multiple poles, and this leads to the presence of logarithmic dependences in the behavior of the total cross sections. The leeway is limited only by the obvious requirement

$$\overline{\sigma}_d \equiv \sigma_{el} \leqslant \overline{\sigma} < \sigma. \qquad (23)$$

It follows from the fact that the entire elastic scattering must (by definition) be included in the kernel of the equation $\overline{\sigma}$, which at the same time is smaller than the total cross section as a result of the fact that all contributions to Eq. (9) are positive. This requirement leads in particular to the result that the power dependence of the cross section on energy turns out to be self-consistent in Eq. (9) only in the case when the leading pole is located at $l<1$, i. e., strictly speaking, an asymptotically constant cross section is inadmissible in the multiperipheral model.[27] It appears that the same requirement fobids also growing asymptotic cross sections in this theory.

In practice, however, the deviation of the pole from the point $l=1$ may be extremely small. Thus, a self-consistent solution of the multiperipheral equations[20] has led to the conclusion that the principal pole lies very close to unity at

$$l = 1 - \varepsilon, \text{ where } \varepsilon = 5 \cdot 10^{-3}. \qquad (24)$$

This means that the cross section will decrease asymptotically in power-law fashion, but with a very small exponent $\epsilon = 5\times 10^{-3}$:

$$\sigma \sim s^{-\varepsilon} \text{ as } s \to \infty. \qquad (25)$$

The question of the pre-asymptotic behavior depends to a considerable degree on the parameters of the kernel $\overline{\sigma}$ of the equation. But in this connection an important role is played by a conclusion deduced in Ref. 20, namely, that to reach the asymptotic regime (25) and to describe the experimental data up to 70 GeV energy it is necessary that $\overline{\sigma}$ decrease weakly with increasing energy in the entire energy interval. This will cause, in particular, all the iterations of $\overline{\sigma}$ to decrease asymptotically weakly with energy, but in the pre-asymptotic region it is possible to have even an increase of the iteration cross sections. This is due to a characteristic feature of the integral term in (9), a feature noted already in Ref. 10, namely that each successive interation leads to accumulation of one more degree of the logarithm of the energy in the behavior of the cross section. Although asymptotically this logarithm is not important, owing to the additional weak power dependence, in the pre-asymptotic region the logarithmic behavior may turn out to be stronger and ensure an increase of the cross section. An example of such a growth was first given in Ref. 28 and was later investigated in detail in the review[29] by Dremin *et al.*

Physically, the growth of the cross section is due to the appearance of new reaction channels. Thus, whereas in the interval from 10 to 100 GeV an important role is assumed in pp interactions by events with two-proton excitations, at energies approximately from 100 to 1000 GeV the contribution of the third-iteration processes, with formation of one pion block between two excited nucleons, becomes already important, and at energies from 10^3 to 10^4 GeV processes with two pion blocks come into play. The masses of these blocks are relatively large, on the order of 3 GeV, and it is this which causes this slow sequence of the iterations (see Ref. 11). These are precisely the pion clusters that were named fireballs.[4)] The appearance of one fireball (energy ~100 GeV) opens up the pre-asymptotic region, and one can expect three fireballs to be sufficient already to reach the asymptotic regime, which consequently sets in at energies ~10^6 GeV. In this energy region, one should expect a noticeably weakening energy dependence, which flattens out and eventually decreases. At the same time, the role of inelastic diffraction also increases, and can contribute, from the multi-

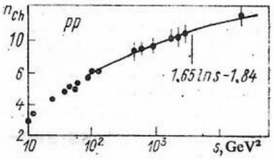

FIG. 6. Dependence of the growth of the average multiplicity of the charged particles on the energy.

peripheral point of view, both directly to the irreducible term of Eq. (9), and to its integral term (owing to the contribution of the elastic scattering $\overline{\sigma}_d$ to the kernel of the equation).

Average multiplicity. The number of secondary particles produced in the collisions increases with increasing energy. This growth is rather weak in comparison with the maximum possible ($\sim s^{1/2}$) and is well approximated by a logarithmic energy dependence (Fig. 6). This dependence is obtained naturally in the multipheripheral theory, [8] when the masses of the blocks are strongly limited and each block emits a finite number of particles. In this case the growth of the multiplicity is due simply to the increase in the number of blocks with increasing energy, which obeys a logarithmic law.

The total-multiplicity growth rate, determined by the coefficient of ln s, depends strongly on the model of the process, i.e., on the mass of the block and on the character of its decay. We note that models in which the block breaks up into the "maximum" number of particles (e.g., statistically with approximate energy 0.4–0.5 GeV per secondary particle in the rest system of the block), lead to a coefficient on the order of 2.5 (Ref. 11), whereas the production of small-mass blocks (say of ρ mesons) or "pheripheral" decay of the blocks themselves (on account of single-particle but not one-pion exchanges) leads usually to a coefficient smaller than or of the order of unity. [16,22,23] Experiment favors a coefficient noticeably larger than unity (see Fig. 6). Therefore in the models of the second type the only way out is to attribute the greater part of the effect to the irreducible (nonperipheral) term, which is frequently represented in the form of a simultaneous formation of two or several parallel multipheripheral chains, and this naturally improves the picture of the distribution with respect to multiplicity.

We note, however, that within the framework of the multiperipheral theory there is also another possible situation, wherein the masses of the blocks are weakly bounded, and the decay of the block itself follows a power law, i.e., the average number of particles in the block increases with its mass in power-law fashion: $\overline{n}_{av} \sim M^a$. In this case a power-law increase of the average multiplicity with energy is possible. These possibilities have not yet been investigated analytically in detail.

Inclusive distributions with respect to the longitudinal momentum. A characteristic feature of inclusive distributions with respect to the longitudinal momentum, one most extensively discussed of late, is scaling. This property is manifest in the fact that at asymptotically high energies ($s \to \infty$) the invariant differential cross sections should, in accordance with a suggestion by Feynman, [30] be functions of the ratio of the longitudinal momentum of the secondary particle to the collision energy in the c.m.s., but not of each of these variables separately, i.e.,

$$Ed^3\sigma/d^3p_{(s\to\infty)} = f(x, p_\perp), \quad (26)$$

where $x = 2p_\parallel/\sqrt{s}$, $(\mathbf{p}, E)$ are the momentum and energy of the secondary particle. Instead of the distribution with respect to the longitudinal momenta, one frequently considers the distribution with respect to the rapidity y:

$$y = -\tfrac{1}{2}\ln[(E+p_\parallel)/(E-p_\parallel)] \quad (27)$$

or, if only the particle emission angles are measured and not their momenta, one uses the distribution with respect to the quantity

$$\eta = \ln[(p+p_\parallel)/(p-p_\parallel)] = \ln \mathrm{tg}\,\theta/2. \quad (28)$$

Therefore, whenever we refer to the quantity y, we shall mean actually η if we deal with experiments in which only the particle emission angles are measured. Even from cosmic-ray experiments it followed that a hierarchy exists in the establishment of scaling at high energies. [31] This has now been confirmed by the CERN colliding-beam experiments. [24] The experiments indicate the presence of three types of secondary particles, [5)] resulting from pionization, fragmentation, and diffraction. By diffraction particles one means quasielastically scattered primary particles with $0.95 \leq x < 1$. Fragmentation particles are those carrying away a finite (as $s \to \infty$) fraction of the momentum of the primary particles. At present-day energies, they are arbitrarily defined as particles with $0.1 \leq x \leq 0.8$. Pionization particles fill the region near $x=0$ and make the largest contribution to the average multiplicity.

In terms of the variable y, the diffraction and fragmentation particles are at the outermost edges of the distribution, whereas the pionization particles occupy the bulk of the space in the y scale. In the fragmentation region, the pions reach scaling most rapidly (already at energies close to 30 GeV). In the pionization region, however, at $x=0$, the pion distributions increase by approximately a factor of two from 30 to 1500 GeV, and it appears that they reach scaling at this energy with an

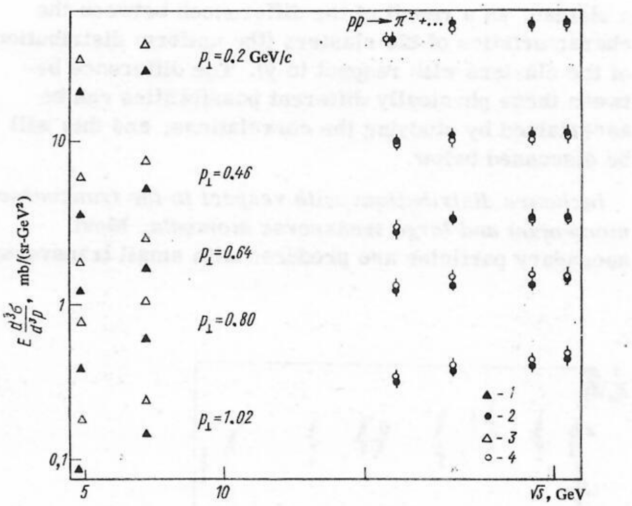

FIG. 7. Approach to scaling of inclusive distributions of pions at $x=0$: 1—Mück *et al.* π^+; 2—Saclay—Strasbourg π^-; 3—Mück *et al.* π^+; 4—Saclay—Strasbourg π^+.

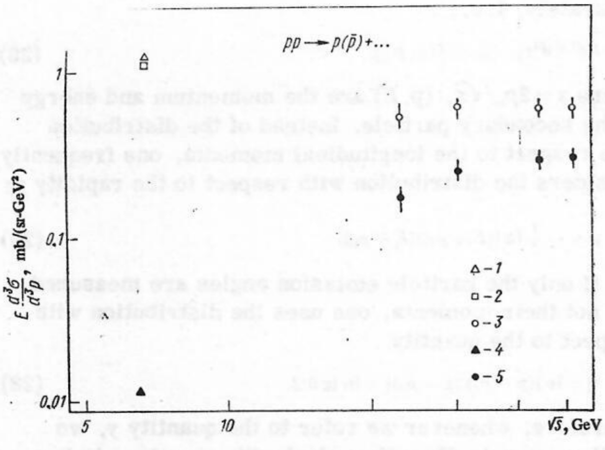

FIG. 8. Approach to scaling of inclusive distributions of antiprotons at $x=0$ and $p_\perp = 0.65$ GeV/c: 1—Allaby *et al* p; 2—Mück *et al.* p: 3—Saclay–Strasbourg $\bar{p}$; 4—Allaby *et al.* $\bar{p}$; 5—Saclay-Strasbourg p.

accuracy on the order of 10% (Fig. 7).[6)] For heavier particles, the approach to scaling is slower than for pions. This is demonstrated in Fig. 8 for antiprotons.

Theoretically, the scaling property follows from many model concepts, and can hardly be used to make the choice between different models that describe inelastic interactions. It is interesting to note, however, that this property was first demonstrated in the multiperipheral scheme[8] for fragmentation particles (constancy of the inelasticity coefficient) and for pionization particles, for which the distribution with respect to y leads to a plateau: $d\sigma/dy = \text{const}$. The presence of this plateau (again, accurate to about 10–15%), was demonstrated in experiment (Fig. 9).

The most interesting problem that arises here is whether the plateau is the result of summation of individual events, each of which has also a uniform distribution in the y scale, or whether the individual events yield uneven distributions of the particles in this scale (clusters or fireballs), which are summed and lead, if the number of events is large enough, again to a plateau, as a result of the differences between the characteristics of the clusters (the uniform distribution of the clusters with respect to y). The difference between these physically different possibilities can be ascertained by studying the correlations, and this will be discussed below.

Inclusive distributions with respect to the transverse momentum and large transverse momenta. Most secondary particles are produced with small transverse

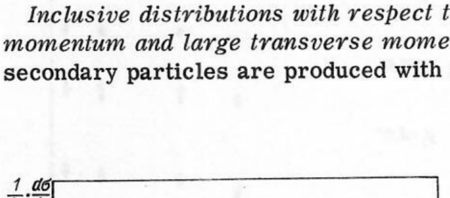

FIG. 9. Plateau in the pion rapidity distribution.

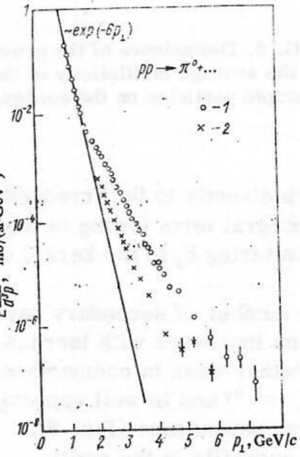

FIG. 10. Distribution of pions with respect to the transverse momenta at $x=0$: 1) $s=1850$ GeV^2; 2) $s=950$ GeV^2.

momenta (the average transverse momentum is on the order of 0.4 GeV/c). In the transverse-momentum region up to 1.5 GeV/c, the differential cross section for pion production decreases exponentially

$$Ed^3\sigma/d^3p \sim \exp(-6p_\perp) \quad (29)$$

(here $p_\perp$ is in GeV/c).

At higher values of the transverse momentum, the number of pions produced turned out to be much larger than expected from a simple extrapolation of formula (29) in this region (Fig. 10).

A weaker decrease of the cross sections with increasing $p_\perp$ was predicted theoretically[32] (before the experiments were performed), as a consequence of electromagnetic effects similar to those observed in deep inelastic interactions of electrons with protons. The observed effect turned out, however, to be stronger by approximately four orders of magnitude, thus indicating that it is of hadronic character.

Processes with large transverse momenta turn out to have interesting properties:

1) The cross section decreases with increasing $p_\perp$ like $p_\perp^{-8}$ (Refs. 33–35) or like $\exp(-10\sqrt{p_\perp})$ (Ref. 36).

2) No scaling is observed in this region even at ISR energies (see Fig. 10).

3) There is no absolute predominance of pions (the fraction of $\pi^+ + \pi^-$ is 55%, $K^+ + K^- \sim 27$, $\bar{p} + p \sim 18\%$) in the charged-particle flux in the transverse-momentum interval from 2 to 3.5 GeV/c.

4) Processes with large transverse momenta are characterized by a large average multiplicity.

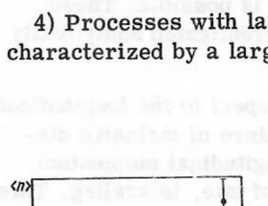

FIG. 11. Dependence of the growth of the number of secondary particles on the growth of the transverse momentum of one of them.

5) The number of secondary particles produced in the process is larger, the larger the registered transverse momentum of one of them (Fig. 11).

6) The number of secondary particles increases in a direction opposite to that of the emission of the registered particle, and slightly in the same direction, i.e., the difference between them also increases.

7) There is a noticeable excess of production of positively charged particles over negatively charged ones (their ratio is approximately 1.3 to 1.4).

The region of small transverse momenta, while undoubtedly of interest, has not been attracting much attention by theoreticians, because in most methods of describing the dependence on the transverse momenta (including the multiperipheral theory) it is necessary to resort to relatively arbitrary form factors and to the parameters associated with them, i.e., the theoretical results turn out to be strongly dependent in this region on the choice of the particular parameters of the model.

At the same time, the description of processes with large transverse momenta depends less on the choice of the model. Although the proposed theoretical schemes[33–37] differ in their details, nonetheless most of them lead to a description of the experiments with the aid of the multiperipheral theory with allowance for the parton structure of the particles. We emphasize that a distinguishing feature of a process with large momentum transfer is that in the multiperipheral theory it is unnecessary in this case to resort to the use of some concrete model for the kernel of Eq. (9), and all the results can be obtained by using merely the properties of the total cross section off the mass shell. Indeed, if at small transverse momenta we consider, for example, one iteration diagram with three blocks, as shown in Fig. 2, then in the case of large momentum transfers, which have a low probability, it is necessary to take into account the fact that this momentum can be transferred by either the upper or the lower of the exchanged particles. Summation of all these possibilities leads to the result[34] that the distribution with respect to the squared 4-momentum transfers can be easily obtained from the integral term in (9), in which $\overline{\sigma}$ need be replaced by σ:

$$\frac{d\sigma_{pp}}{dk^2}=\frac{1}{16\pi^3 s^2}\frac{1}{(k^2-\mu^2)^2}\int(s_1+k^2)\,\sigma_{\pi p}(s_1,k^2)\,ds_1 \times\int(s_2+k^2)\,\sigma_{\pi p}(s_2,k^2)\,ds_2. \quad (30)$$

The role of the parton structure of the proton becomes clear if it is assumed that the virtual pions behave off the mass shell in analogy with virtual photons. Then, using the known properties of the cross sections for interaction of the virtual photons[38,39] we can write

$$\sigma_{\pi p}(s_i,k^2)=\sigma_{\pi p}\frac{s_i}{s_i+k^2}\frac{1}{1+\beta k^2}\cdot\frac{1}{1+\gamma k^2}, \quad (31)$$

where $\sigma_{\pi p}\approx 24$ mb is the πp-interaction cross section on the mass shell; the parameters $\beta = 0.035\ \text{GeV}^{-2}$ and $\gamma\approx(s_0-M^2)^{-1}\approx 3.3\ \text{GeV}^{-2}$ are known from ep experiments,[38,39] where we neglect the particle masses. From (30) and (31), taking into account the condition that determines the integration region

$$(s_1+k^2)(s_2+k^2)\leqslant sk^2. \quad (32)$$

we readily see that the distribution with respect to the momentum transfers will decrease in power-law fashion like $(k^2)^{-4}$. Indeed, the $(k^2)^{-2}$ factor is due to the propagator, $(k^2)^{-4}$ to the product of the cross sections, and $(k^2)^2$ to the phase space, i.e., the integration limits in (32). Allowance for the decay of each of the blocks is simple and leads to a pion distribution proportional to $p_\perp^{-8}$. Since all the parameters are specified, the absolute normalization is also established. The result describes adequately the experimental data (for details see Ref. 34) on the distribution of the pions with respect to the transverse momenta (Sec. 1) and its energy dependence (absence of scaling, Sec. 2).

The large fraction of the heavy particles can be explained by taking into account at large $p_\perp$ the exchange of particles of this kind, inasmuch as the role of the particle masses in the propagators is no longer small (large k^2!) and everything is determined by the vertex parts [the cross sections under the integral sign in (30)] and by phase space.

The picture developed above also explains naturally the fourth and fifth properties of the process. The presence of the factor $s_i/(s_i+k^2)$ in (31) suppresses the small masses at large momentum transfers, i.e., increases the multiplicity of the process the more, the larger k^2, and hence also $p_\perp$.

However, the explanation of the last of the aforementioned properties leads to difficulties, since positively charged particles can predominate in this model, with equally probable exchange of all the charges only as a result of the primary positive charge of the colliding particles. It is not clear, however, whether this circumstance can ensure the required ratio of the number of positive to negative particles, which equals 1.3 according to the preliminary data.

Processes with large momentum transfer are always of interest, since they raise hopes of studying the structure of particles at short distances. In Ref. 37 it is shown, with the properties of multiperipheral models of the $\lambda\varphi^3$ type as an example, that inclusive events such as deep inelastic ep collision and production of pions with large transverse momenta serve as a check on the hypothetical existence of pointlike constituent particles in hadrons (partons), whereas exclusive processes such as elastic (hadron-hadron or lepton-hadron) scattering with large $|t|$ are determined mainly by the manner in which the hadron is made up of these constituents. Similar conclusions follow from the assumption that each hadron is a reggeizing bound state of several elementary constituents and is described by a ladder of the $\lambda\varphi^3$ type. The physical cause of this correspondence appears to be more general than the various particular models. It lies in the fact that in inclusive processes with large momentum transfer this transfer is "felt" actively by a minimum number of constituents, so that the type of these constituents is more significant than their number.

In exclusive elastic-scattering processes, to the contrary, it is important that the initial bound particle,

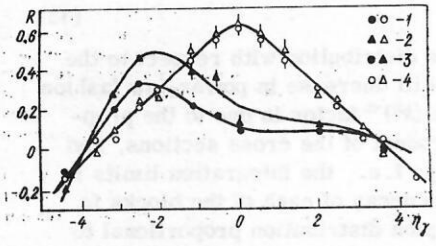

FIG. 12. Correlations between neutral and charged pions: 1) $\sqrt{s}=30.6$ GeV; 2) $\sqrt{s}=53$ GeV; 3) charged particles; 4) neutral particles;

after acquiring the large momentum, be "gathered together" again, and this is more difficult, the larger the number of constituents, i.e., the character of the elastic scattering depends on the internal structure of the bound state, and in particular on the number of its constituent partons.

Thus, further study of these processes will undoubtedly add much to our understanding of the internal structure of the particles.

Two-particle correlations. The single-particle inclusive distributions serve as information, averaged over many parameters, concerning the processes. More detailed information can be obtained by studying the correlations between the produced particles. But this raises a problem connected with the large number of possibilities, for even a system of two particles involves already six variables dependent on the momentum alone, in addition to requiring information on the particle charges, their nature, etc.

At present the most popular activity is the study of the correlations between the longitudinal momenta of two secondary particles[7)] by comparing the two-particle distributions $d^2\sigma/dy_1\,dy_2$ with the corresponding single-particle distributions $d\sigma/dy_1$ and $d\sigma/dy_2$. This comparison is made most frequently with the aid of the correlation function

$$R(y_1, y_2)=\sigma_{in}\frac{d^2\sigma/dy_1dy_2}{d\sigma/dy_1\cdot d\sigma/dy_2}-1. \qquad (33)$$

The experimentally measured correlation functions are given in Fig. 12, which shows the correlation between the charged pions and neutral pions (decay γ rays) at energies $\sqrt{s}=31$ and 53 GeV. The rapidities of the charged pions were fixed ($y_1=0$ and -2.5). We see that in both cases the neutral pions are emitted predominantly with the same values of rapidity. Effects of this type, when particles with close values of rapidity are correlated, are called short-range correlations. At the same time Fig. 12 shows a noticeable difference between the correlation function for small rapidities ($y_1=0$) and the case when the charged-pion rapidity is taken in the fragmentation region ($y_1=-2.5$). This is the consequence of the long-range correlations.

Usually the function R is approximated in the region of the short-range correlations by an exponential with a correlation length $\lambda=2$. This picture appears, naturally, in the reggeon technique developed by Mueller and Kancheli, where the quantity $\lambda=2$ is determined by the intersection of the trajectories closest to the vacuum trajectory.

It must be emphasized that the correlation function in the neutral region is equal to approximately 60–70% (i.e., $R\approx 0.6-0.7$). This is a rather large value.

All these characteristics are quite important for the choice between the various theoretical schemes. Thus, the limiting-fragmentation model[40] leads to a constant number of clusters whose dimensions increase appreciably with increasing energy. In this case the two-particle correlations should increase with increasing energy, since the particle density increases in definite regions on the rapidity scale. Since in experiment the pionization component plays clearly a significant role and the indicated growth of the correlation function is not observed, it follows that the simplest model of limiting fragmentation does not agree with experiment.

In the multiperipheral models the number of produced blocks (clusters) increases with energy. It can be shown that the correlation function should approach a constant limit, as is indeed noted in experiment. But different models yield different values of the cluster mass, and hence of the correlation function. Thus, if we take the simplest model[8] with ρ-meson production, then it turns out[41] that (on top of the shortcoming connected with the asymptotically rapid decrease of the cross section) this model leads to too small a value of the correlation function, only about 10% at the maximum. To obtain the required value (~60–70%) it is necessary to postulate the presence of clusters that decay to produce approximately five charged particles.[41] This is approximately the number obtained from fireball theory,[11] where the conclusion that such clusters (fireballs) are produced followed from the requirement that the total cross section be practically constant at very high energies (that the leading singularity in the l plane be close to unity).

Part of the formation of the correlation-function maximum is attributed in Ref. 41 to the presence of long-range correlations connected with inelastic-diffraction processes. However, even at the maximum possible correlations of this type it is impossible to obtain the required value of the correlation function without assuming the production of clusters that break up into several particles.

Thus, the data on the correlations of secondary particles seem to favor the picture in which clusters are produced and break up into a rather large number of particles, and the number of these clusters increases with increasing energy. The question of the degree to which these clusters coincide with the fireballs observed in cosmic radiation [see (15) and (31)] is undoubtedly worthy of further research.

One of the most essential questions here involves the role of the long-range correlations and the determination of the correlation function from formula (33). The point is that, as will be discussed in greater detail below, processes in which practically no secondary particles are observed at large angles (with small longitudinal momenta or x) also become significant in this case. Therefore the registration of one of the particles at a large angle already predetermines the choice of

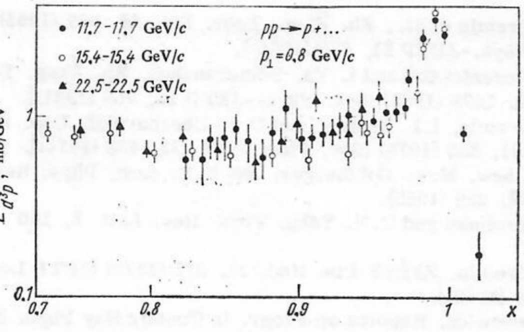

FIG. 13. Proton spectrum at $p_\perp = 0.8$ GeV/c.

some class of processes from among all the possible inelastic events (long-range correlations), so that it is quite possible that we must choose as the normalization coefficient in (33) not the total inelastic cross section, but only a fraction of it. We see therefore that the question of the reality of the clustering, the size of the clusters, and their description in the multiperipheral model is closely related with other processes and with the determination of the correlation function. Independent methods of investigating this problem would be quite desirable.[8)]

Inelastic diffraction. Inelastic diffraction processes are usually defined as processes in which one of the colliding nucleons remains unexcited, and the other goes into an excited state having the same quantum numbers and decaying subsequently with emission of a relatively small number of secondary particles. The existence of such unexcited nucleons is clearly seen in the nucleon spectrum at ISR energies, in which a quasielastic peak is clearly pronounced at $x > 0.95$ (Fig. 13). In principle it is possible to have diffraction processes in which both nucleons are excited without a change in their quantum numbers, but it would be appreciably more difficult to observe them and to separate them from the remaining events.

The problem of excitation of even one of the nucleons cannot be regarded as solved, since usually no complete study is made of the quantum numbers of the excited state. Therefore not all the events that contributed to the quasielastic peak can be attributed to inelastic diffraction, and measurement of the total cross section in this region yields only the upper bound of the cross section of the inelastic diffraction interaction. An estimate given in Ref. 24, which involves furthermore a certain leeway in the extrapolation of the experimental data to the region of small transverse momenta, yields for this limit a value equal to the total elastic cross section of the scattering. It should be noted that a noticeable contribution to this cross section is made also by processes with relatively large excitation masses of the second nucleon (approximately up to 10 GeV). One cannot therefore say that the excitation spectrum is strongly bounded in diffraction processes, although the multiplicity in these processes is still patently less than average.

Such processes lead to a strongly collimated jet of secondary particles,[24] with practically no particles having small values of x and y. As already mentioned, the determination of the role of these processes is important also for the solution of the problem of particle clustering.

The investigation of these events is important also from the theoretical point of view for the determination of the pomeron interaction parameters. In diagram language, the inelastic-diffraction process is due to pomeron exchange between the quasielastically scattered nucleons and the diffraction-excited system. At high energies, when the excitation masses are large, the size of the quasielastic peak is connected with a three-pomeron interaction vertex. An estimate[43] based on experimental data and on the use of formulas that follow from the reggeon technique developed by Mueller and Kancheli, has led to a small value of this vertex at $t=0$, namely $g_p(0) \approx 0.2$ GeV^{-1} (for example, the pomeron-particle interaction constant is of the order of the square root of the total cross section, i.e., about 5–10 GeV^{-1}).

In the multiperipheral theory this quantity can be calculated from other considerations.[44] If the entire "ladder" constructed for the nucleus without allowance for elastic diffraction, i.e., $\overline{\sigma} = \sum \overline{\sigma}_r + \overline{\sigma}_b$ is compared with the leading pole, and the diffraction term is regarded as a perturbation, then this perturbation corresponds to a cladding of the leading singularity, i.e., to a three-pomeron vertex:

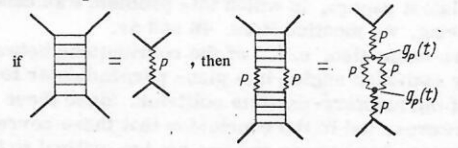

The use of the equations given in Sec. 1 and of the ensuing parameters of the behavior of the total cross sections allows us to estimate the three-pomeron vertex[44] as $g_p(0) = 0.15$ GeV^{-1}. It follows therefore that the multiperipheral theory describes correctly also the quasielastic peak in the proton spectrum. The difference between the three-pomeron vertex and zero is uniquely connected with the asymptotic decrease of the cross sections, and the smallness of the vertex is due to the weakness of this decrease (smallness of ϵ!), as already discussed in Sec. 1.

CONCLUSION

The purpose of this review was to demonstrate the correspondence between different models within the framework of the multiperipheral approach and to compare them with the experimental data at high energies. For the sake of brevity, all mathematical derivations were omitted and the emphasis was on a clarification of the qualitative consequences of the theory and their agreement with experiment. The reader can find the details of the calculations in the references. Practically no references are made to experimental work, since the author has guided himself mainly by the results of encounters between experimenters and theoreticians at CERN, which were reported in Jacob's review.[24]

The status of theory and experiment at present is still such that many premises are still not rigorously proved or verified, and further work is needed to clarify the characteristic features of inelastic processes. It is nevertheless obvious that the main qualitative features known from cosmic-ray physics[15,31] are confirmed and further developed by the ISR experiments. The immeasurably abundant information obtained in these experiments permits a deeper knowledge of the processes and can lead to a qualitatively new stage. The multiperipheral theory does not encounter here any difficulties when it comes to describing the main qualitative characteristics of the processes, although there is still a long way to go before it can be quantitatively compared with all the data.

1) i.e., the part that does not contain two-particle intermediate states in this channel.

2) We shall not discuss here the role of the interference terms, referring the reader interested in this problem to the review.[11]

3) Other parameters were given in the fit formulas of certain papers, but the constant term varied in all of them within about 1—2%, and the coefficient of the square of the logarithm ranged from 0.4 to 0.68.

4) We shall return to the question of pion clustering in the section devoted to the correlation of secondary particles.

5) It should be emphasized that this subdivision is still quite arbitrary and has no distinct boundaries (see below).

6) We shall not dwell in detail on the character of the approach to scaling, which has been analyzed in many papers. From among the latest papers, in which this problem was connected with clustering, we mention Refs. 46 and 51.

7) Studies were made also, e.g., of the correlations between the particle emission angles in a plane perpendicular to the direction of the primary-particle collision. Since these studies, however, led to the conclusion that these correlations are due to phase space and are not too critical to the dynamics of the process, we shall not stop to discuss them here.

8) We note in this connection a method proposed in Ref. 42 for the study of correlations by determining the squares of the 4-momentum transfers; this method calls for the performance of exclusive experiments with complete information on the momenta of all the secondary particles and is particularly effective if any one particular mechanism predominates.

1 G.T. Zatsepin, Dokl. Akad. Nauk SSSR **67**, 933 (1949).
2 E.L. Feĭnberg and D.S. Chernavskiĭ, Dokl. Akad. Nauk SSSR **81**, 795 (1951); **91**, 511 (1953).
3 D.I. Blokhintsev, Proc. of CERN Symposium, Vol. 2 (1956), p. 155.
4 G. Goebel, Phys. Rev. Lett. **1**, 337 (1958).
5 G.F. Chew and F.E. Low, Phys. Rev. **113**, 1640 (1959).
6 I.M. Dremin and D.S. Chernavskiĭ, Zh. Éksp. Teor. Fiz. **38**, 229 (1960) [Sov. Phys.-JETP **11**, 167 (1960)].
7 F. Salzman and G. Salzman, Phys. Rev. Lett. **5**, 377 (1960); Phys. Rev. **120**, 559 (1960).
8 D. Amati *et al.*, Nuovo Cimento **22**, 569 (1961); **26**, 896 (1962).
9 I.M. Dremin *et al.*, Zh. Éksp. Teor. Fiz. **48**, 952 (1965) [Sov. Phys.-JETP **21**, 633 (1965)].
10 V.B. Berestetskiĭ and I. Ya. Pomeranchuk, Zh. Éksp. Teor. Fiz. **39**, 1078 (1960) [Sov. Phys.-JETP **12**, 752 (1961)].
11 I.M. Dremin, I.I. Roĭzen, and D.S. Chernavskiĭ, Usp. Fiz. Nauk 101, 385 (1970) [Sov. Phys.-Usp. **13**, 438 (1971)].
12 G.F. Chew, M.L. Goldberger, and F.E. Low, Phys. Rev. Lett. **22**, 208 (1969).
13 S.B. Treiman and C.N. Yang, Phys. Rev. Lett. **8**, 140 (1962).
14 I.M. Dremin, ZhÉTF Pis. Red. **11**, 272 (1970) [JETP Lett. **11**, 178 (1970)].
15 M. Miesowicz, Reports on Progr. in Cosmic Ray Phys. **10** (1970).
16 D.M. Tow, Phys. Rev. **D2**, 154 (1970).
17 K.G. Boreskov, A.B. Kaĭdalov, and L.A. Ponomarev, Preprint ITÉF, 950 (1972).
18 G.F. Chew, T. Rogers, and D.R. Snider, Phys. Rev. D2, 765 (1970).
19 G.F. Chew and D.R. Snider, Phys. Rev. **D1**, 3453 (1970).
20 E.I. Volkov *et al.*, Yad. Fiz. **17**, 407 (1973) [Sov. J. Nucl. Phys. **17**, 208 (1973)].
21 H.D.I. Abarbanel *et al.*, Phys. Rev. Lett. **25**, 1735 (1970).
22 E.M. Levin and M.G. Ryskin, Phys. Lett. **B41**, 626 (1972).
23 E.M. Levin and M.G. Ryskin, Yad. Fiz. **17**, 386 (1973) [Sov. J. Nucl. Phys. **17**, 199 (1973)].
24 M. Jacob, Preprint Ref. TH. 1639-CERN; LAL-PUB-73/18-THY (1973).
25 K.A. Ter-Martirosyan and K.G. Boreskov, ITÉF Preprint No. 867 (1971).
26 I.V. Andreev, Yad. Fiz. **14**, 837 (1971) [Sov. J. Nucl. Phys. **14**, 468 (1972)].
27 I.I. Roĭzen, in: Nucleons and Pions [in Russian], Dubna (1968).
28 V.N. Akimov *et al.*, Yad. Fiz. **7**, 629 (1968) [Sov. J. Nucl. Phys. **7**, 389 (1968)].
29 I.M. Dremin, I.I. Roĭzen, and D.S. Chernavskiĭ, Trudy FIAN SSSR, **57**, 117 (1971).
30 R.P. Feynman, J. Phys. Rev. Lett. **23**, 1415 (1969).
31 E.L. Feinberg, Phys. Rev. **C5**, 237 (1972).
32 S.M. Berman, G.D. Bjorken, and J.B. Kogut, Phys. Rev. **D4**, 3388 (1971).
33 D. Amati, L. Caneschi, and M. Testa, Phys. Lett. **B43**, 186 (1973).
34 I.M. Dremin, Yad. Fiz. **20**, 149 (1974) [Sov. J. Nucl. Phys. **20**, 78 (1975)].
35 E.M. Levin and M.G. Ryskin, Yad. Fiz. **20**, 519 (1974) [Sov. J. Nucl. Phys. **20**, 280 (1975)].
36 J. Harte, Yale University Preprint (1973).
37 D. Amati, L. Caneschi, and M. Testa, Preprint Ref. TH. 1644-CERN (1973).
38 J.W. Moffat and V.G. Snell, Phys. Rev. **D3**, 2848 (1971).
39 I.M. Dremin, Yad. Fiz. **15**, 582 (1972) [Sov. J. Nucl. Phys. **15**, 322 (1972)].
40 J. Benecke *et al.*, Phys. Rev. **188**, 2159 (1969).
41 P. Pirila and S. Pokorski, CERN Preprint TH-1607 (1972); Phys. Lett. **B43**, 502 (1973).
42 I.M. Dremin and D.S. Chernavskiĭ, Yad. Fiz. **14**, 469 (1971) [Sov. J. Nucl. Phys. **14**, 263 (1972)].
43 A.B. Kaidalov *et al.*, Phys. Lett. **B45**, 493 (1973).
44 H.D.I. Abarbanel *et al.*, Ann. Phys. (N.Y.) **73**, 156 (1972).

Translated by J. George Adashko